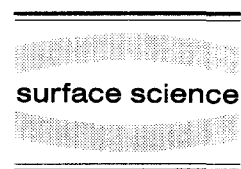




ELSEVIER

Surface Science 335 (1995) 361–371



Surface and electrochemical characterization of electrodeposited PtRu alloys

Frank Richarz, Bernd Wohlmann^{*}, Ulrich Vogel, Henning Hoffschulz, Klaus Wandelt

Institut für Physikalische und Theoretische Chemie, Universität Bonn, Wegelerstrasse 12, D-53115 Bonn, Germany

Received 12 January 1995; accepted for publication 9 February 1995

Abstract

PtRu alloys of different compositions were electrodeposited on Au. Twelve alloys between 0% and 100% Pt were characterized with surface sensitive spectroscopies (XPS, LEIS) after transfer from an electrochemical cell to an ultra high vacuum chamber without contact to air. The composition of the thus prepared alloys showed a linear dependence on the concentrations of the deposition solution, but was Pt-enriched both in the bulk and (even more so) at the surface. During the electrochemical reduction of the metal cations, sulfur from the supporting electrolyte 1N H₂SO₄ was found to be incorporated into the electrodes. Cyclic voltammetry was used for the determination of the electrocatalytic activity of the electrodes for the oxidation of carbon monoxide. The highest activity for this oxidation as measured by the (peak) potential of the CO oxidation cyclovoltammograms was found for a surface concentration of ~ 50% Pt. The asymmetry of this “activity curve” (oxidation potential versus Pt surface concentration) is tentatively explained in terms of a surface structural phase separation.

Keywords: Carbon monoxide; Catalysis; Electrochemical methods; Low energy ion scattering (LEIS); Oxidation; Platinum; Ruthenium; Solid–liquid interfaces; X-ray photoelectron spectroscopy

1. Introduction

Up to now PtRu alloys seem to be the favorite choice for the anode material in direct (DMFC) and indirect (IMFC) methanol fuel cells. Both cells are in principle very attractive energy sources to be used in mobile systems, because the fuel is liquid at room temperature and the cells are operating at rather low temperatures (below 100°C) compared to phosphoric acid fuel cells. These low temperatures prevent the emission of NO_x or hydrocarbons and are a neces-

sary prerequisite for the use of solid polymer electrolyte cells.

In spite of these obvious advantages both the DMFC and the IMFC are not yet ready for technical applications at the present stage of development. Among others, the main problem is the poisoning of the electrodes by carbon monoxide or other adsorbates. In the direct oxidation of methanol CO was found as a strongly adsorbing reaction intermediate [1]. For the IMFC the fuel is produced from methanol via a reforming process and contains ~ 74% H₂, ~ 23% CO₂ and up to a few percent carbon monoxide [2]. This hydrogen-rich fuel passes the anode and CO impurities are adsorbed on the Pt, thereby block-

^{*} Corresponding author. Fax: +49 228 732551.

ing the adsorption sites needed for the main reaction, namely the hydrogen oxidation, and thus decreasing the efficiency of the cell dramatically. In principle the CO can be removed by much higher working temperatures of the cell, but hot acid electrolytes are not usable in mobile electrochemical cells for several reasons.

It is this poisoning problem which can be reduced by using a PtRu alloy anode instead of pure Pt. The use of an PtRu anode leads to a lowering of the CO oxidation potential and, as a consequence, to an enhanced CO tolerance [3], a lower poisoning rate [4] and higher activity for the hydrogen oxidation [5] than of pure Pt electrodes.

This behavior is commonly explained in terms of the so-called bifunctional mechanism which was first proposed by Watanabe and Motoo [6]. This mechanism is based on the presence of an oxygen containing species on Ru at much lower potentials than on Pt. This was confirmed by Ticanelli et al. [7], who found an oxygen containing adsorbate already at potentials as low as 250 mV versus RHE (reversible hydrogen electrode). The existence of this reaction partner enables the CO oxidation at lower potential. The most favorable alloy composition for this process was proposed to be a 50:50 mixture in the surface, in which each Pt atom should have a direct Ru neighbor, which delivers the oxygen species [6]. In contrast to this pure geometric argument, which relies on a uniform distribution of both alloy components, some authors refer to an additional electronic effect due to alloy formation. The electronic structure of the Pt atoms in the alloys should be different from that in pure Pt. As a consequence the interaction between Pt and CO should also be altered. However, as yet no direct evidence for the existence of this electronic effect has ever been presented.

Up to now PtRu alloys were studied in two directions, as real catalyst materials by more technically relevant methods or as model electrodes in more basic studies. Very different types of alloy samples were used and the preparation methods were manifold. Some of the authors worked with bulk alloys, either commercial [8] or homemade [14,7] samples, others used a reductive codeposition of the constituent, either chemical [3,9] or electrochemical [10]. Another very common preparation method is the deposition of Ru on a Pt substrate with different

sizes of the Ru particles [6,11]. The catalysts closer related to application were mostly prepared by impregnation with the metal salts on high surface area substrates such as pyrographite-coated carbon fibre paper [4]. Additionally some exotic preparation methods like the implantation of Ru in Pt by ion bombardment [12] or the spraying of a mixture of the metal oxides in toluene onto a Au substrate [13] were used. With the exception of the work by Gasteiger et al. [14–18] the composition of the outermost electrode layer remained unknown in most of these former investigations. Most of the researchers developed some kind of “activation” of their electrodes by heating them in a gas stream or by reducing or oxidizing them to some extent in the electrolyte. Even if the surface composition of the alloy would have been known at the beginning of the studies these activation procedures are known to *alter* the surface properties; heating results in the segregation of either Pt or Ru [19] depending on the gas atmosphere while Ru oxides are easily formed at potentials above 950 mV versus RHE up to loss of Ru through corrosion above 1.3 V versus RHE [7]. Therefore the surface composition has to be checked *after* “activation” and can clearly not be extrapolated from the bulk composition. Furthermore, in most of the investigations only one or two different alloy compositions were used and compared with the pure metals; the full composition range was never systematically investigated. Gasteiger et al. [14–18] used UHV prepared bulk alloys, but they were limited to a few compositions only and, moreover, had to be transferred through air between the UHV and the electrochemical cell.

In summary, the current picture of the PtRu anode system is the following. The addition of Ru decreases the overpotential for the CO oxidation on Pt (the thermodynamic value is ~ 100 mV versus RHE). The best Ru surface concentration for the CO oxidation was proposed [6,7] and measured [16] to be 50%. In contrast, the best Ru surface concentration for the methanol oxidation was found to be only 7–30% [15,18]. This was explained by the need of three neighboring Pt sites for the dissociative adsorption of methanol. The segregation behavior of the alloys was shown to be strongly dependent on the surrounding gas phase. In UHV [20] and in a hydrogen gas stream [19] a heating of the electrodes

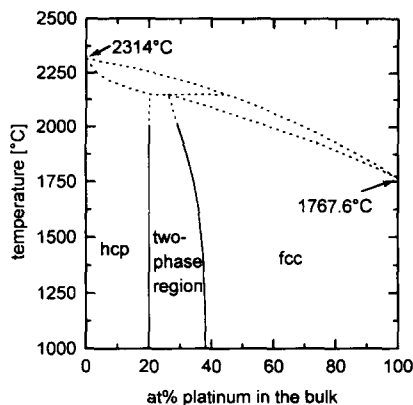


Fig. 1. Phase diagram of Pt and Ru reproduced after J.M. Hutchinson [21].

results in a Pt enrichment at the surface. By contrast, Ru segregation was observed in an oxygen gas stream at 300°C [19]. At potentials higher than 950 mV versus RHE the alloy electrodes are modified first by an irreversible oxidation and later by the loss of Ru. The phase diagram of the PtRu system [21] (Fig. 1) is rather simple, with an fcc phase at Pt concentrations above 40%, an hcp phase at Pt concentrations below 20% and a two-phase region in between.

In order to avoid the above mentioned difficulties in earlier investigations of the PtRu system and to extend the range of surface compositions in this work, we have used the method of electrochemical codeposition of Pt and Ru followed by in situ electrochemical and ex situ surface spectroscopic characterization in an air-free two-chamber transfer apparatus. By means of the electrochemical codeposition it was easy to vary the alloy composition by using mixed solutions of the appropriate metal concentrations as will be described in the following sections. After all, fourteen PtRu electrodes with twelve different surface compositions are prepared in this work and their surface compositions, as determined by X-ray photoelectron spectroscopy (XPS) and low energy ion spectroscopy (LEIS), are directly related to their electrochemical behavior, as characterized by cyclic voltammetry (CV) with and without adsorbed CO. At no stage the surfaces were exposed to air; the only gas which got in contact with the samples was highly purified argon.

From these very systematic measurements with an

unprecedented large number of *known* alloy surface compositions we arrive at a more complete and reliable picture of the electrocatalytic properties of PtRu electrodes towards CO removal by oxidation and at a tentative explanation of its dependence on surface composition based on a surface structural phase transition.

2. Experimental setup

The experiments were carried out in a two-chamber system allowing sample transfer between atmospheric pressure and ultra high vacuum (UHV), the two chambers being separated by a gate valve. This enabled venting the high pressure side with argon up to a slight overpressure or to change samples without destroying the UHV in the main spectrometer chamber. An electrochemical glass cell containing the electrolyte is introduced into the vented high pressure chamber through a second gate valve at the bottom of this chamber. The electrochemical cell is of the flow cell type allowing the electrolyte to be exchanged under potential control. All potentials given in this work refer to the reversible hydrogen electrode (RHE) of the Vogel–Will-type, described in Ref. [22]. Two Pt foils of 1 cm² each are mounted in this cell. They serve a dual purpose. Firstly, the cleanness of the electrolyte is checked by using one of the Pt foils as working and the other one as counter electrode and recording a cyclic voltammogram. Secondly, excessive current densities during deposition are avoided by using the two Pt foils as a pair of parallel counter electrodes.

The electrolytes (see next section) are deaerated with purified argon. A CO saturated electrolyte is produced and kept in store in a glasstube filled with Raschig rings under a permanent stream of CO. The pressure balance between the hydrostatic pressure of the electrolytes and the gas pressure of the permanent argon flow in the chamber is regulated by a glass leak valve in the electrolyte supply tube to maintain a constant electrolyte level in the cell. The electrochemical cell and all the tubings used for electrolyte supply are made of glass (Schott Duran) or Teflon, except the silicone hoses used inside the cell transfer mechanism. The function generator and the potentiostat for the electrochemical measure-

ments are homemade and connected to an AT-compatible PC for digital data collection.

After removal of the electrochemical cell and closure of the gate valve the high pressure chamber is first evacuated to a pressure of less than 10^{-2} mbar by a two-stage rotary pump with a zeolite adsorption trap and an additional liquid nitrogen cooled trap to remove the main part of the water vapor. A further pump down of this chamber is then performed by a 360 ℓ /s turbomolecular pump and a liquid nitrogen cooled titanium sublimation pump. When a pressure of less than 10^{-6} mbar is reached, the respective electrode, mounted on a specially constructed sampleholder, is transferred to the UHV chamber. By this procedure a rather quick sample transfer is achieved, and the first spectrum is typically recorded within 10 min after emersion from the electrochemical cell.

A base pressure of 10^{-10} mbar in the UHV chamber is reached by means of an ion getter pump and a titanium sublimation pump. For surface analysis a hemispherical energy analyzer (SPECS EA10 plus) is used. The analyzer can be polarized either for electron and ion detection. A twin anode X-ray source (VG XR2E) is used for X-ray photoelectron spectroscopy (XPS) and a modified differentially pumped ion gun (Varian) serves as the source for the ions in low energy ion spectroscopy (LEIS). Thermal desorption spectroscopy (TDS) and gas analysis is performed with a quadrupole mass analyzer (VG Q6). In the UHV chamber the sampleholder is mounted on a 5 axis, long z-travel manipulator (VG Omniax 600). The sample can be cooled by liquid nitrogen down to 130 K and heated by a resistance heater up to 1400 K.

All XPS data were collected using Mg K α radiation and a detection angle of 50° off the surface normal. This detection angle somewhat enhances the surface sensitivity compared to normal emission and limits it to 4–5 monolayers. The spectra were recorded in the constant analyzer energy mode (CAE) and the spectral resolution was 0.9 eV. The binding energies for pure Pt 4f $_{7/2}$ and pure Ru 3d $_{5/2}$ are 71.2 and 280.05 eV, respectively.

LEIS data were collected with 2 keV He ions at a scattering angle of 122° (see inset in Fig. 7). The sample was mounted perpendicular to the analyzer. Ion currents of 400 nA/cm 2 were typically used.

The LEIS measurements were quantified by using the signals of the pure metals as a standard in the following formula for binary alloys [23]:

$$X_{\text{Pt}} = \left(1 + \frac{N_{\text{Ru}} S_{\text{Pt}} I_{\text{Ru}}}{N_{\text{Pt}} S_{\text{Ru}} I_{\text{Pt}}} \right)^{-1}, \quad (1)$$

Where X_{Pt} is the molar fraction of Pt in the surface, N_x the surface density of the pure metal standard, S_x the signal of the pure metal standard, and I_x the signal of the metal in the alloy. The standard values were acquired from measurements of pure Pt and Ru during this study.

3. Electrode preparation

PtRu films with a thickness of several μm are produced by electrochemical reduction of the metal cations on a Au substrate. A 0.2 mm thick Au foil was polished with diamond paste with grain sizes down to 1 μm to obtain a mirror finish. After degreasing the foil in boiling saturated KOH solution the substrate was cleaned in millipore water, dried and immediately introduced into the electrochemical chamber.

The solutions from which the alloys were deposited contained variable concentrations of H $_2$ PtCl $_6$ and RuCl $_3$ (both Degussa) in 1N H $_2$ SO $_4$ (Merck suprapur) with a total metal content of 10 mg/ml. The Au substrate was immersed in the deposition solution at a potential of 50 mV and held at that potential for 1 h. After emersion under potential control the electrolyte was exchanged with 1N H $_2$ SO $_4$. During the deposition a continuous stream of Ar was flowing above the solution.

4. Results and discussion

All results presented here were collected following the same experimental procedure. The electrodes were prepared as mentioned above and characterized first by cyclic voltammetry in 1N H $_2$ SO $_4$ electrolyte and by some CO oxidation experiments. After the transfer to the UHV chamber the *surface* compositions of these deposited electrodes were then analyzed by means of XPS and LEIS. Subsequently the

electrodes were sputtered. Since the sputter rates of Pt and Ru are rather similar [14] the final surface composition after excessive sputtering should be close to the *bulk* composition of the deposited films. In any case, these sputtered samples represent electrodes with *new, different surface compositions*, and

were reimmersed in the electrolyte and reinvestigated with cyclic voltammetry and CO oxidation experiments. As a result of this procedure all in all as many as 14 electrodes with 12 different surface composition could be characterized with respect to their electrochemical activity.

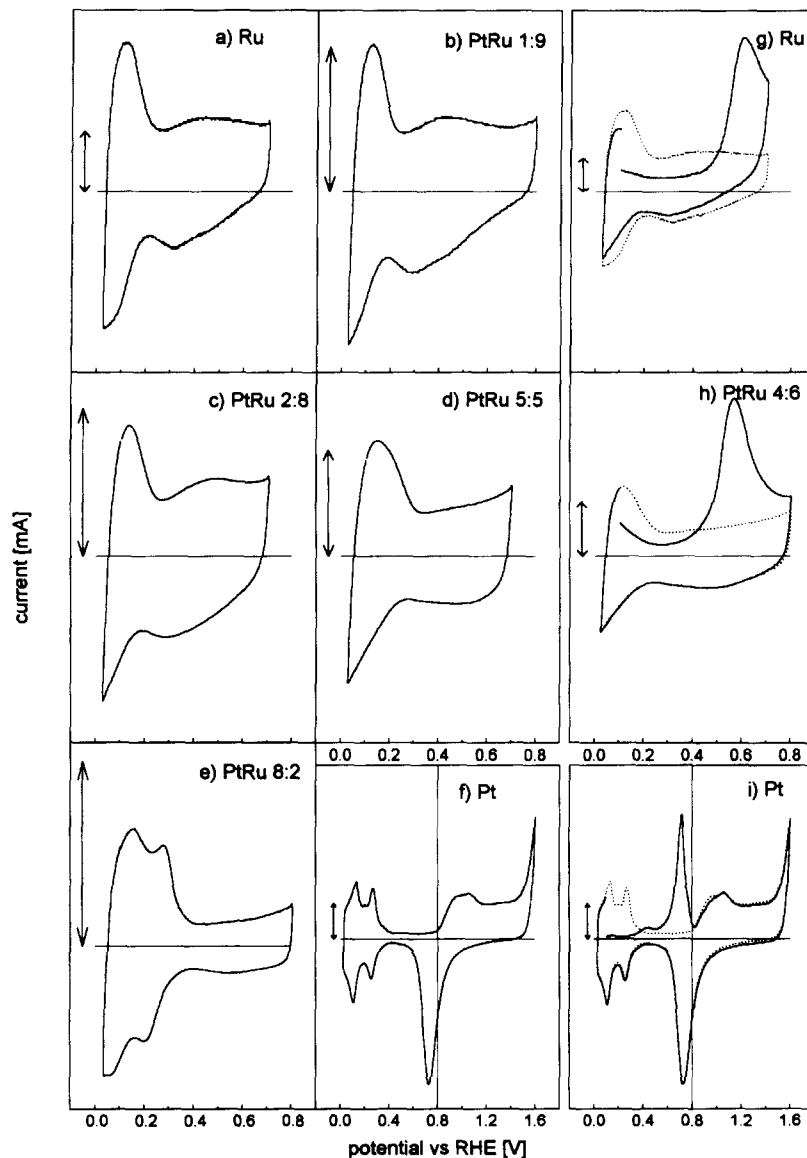


Fig. 2. (a)–(f) Cyclic voltammograms of different PtRu alloys in 1N H₂SO₄ with increasing Pt amount. (g)–(i) CVs with preadsorbed CO in the same electrolyte. (Sweep rate: 20 mV/s, adsorption at 100 mV, CO was removed from the solution). The vertical line at 0.8 V in panels (f) and (h) are optical guides for the comparison with the *reduced* width of the CVs in all other panels. The vertical arrows indicate a current of 10 mA.

4.1. Codeposited electrodes

For a systematic survey of the complete range of compositions we have deposited alloys from solutions with 100, 80, 60, 50, 40, 20, 10 and 0 at% Pt. The electrodes are specified by this composition in the following sections (e.g. PtRu4:6 is the label for an electrode produced from a deposition solution with 40% Pt). Note, however, that neither the bulk composition nor the surface composition of the deposited alloys is necessarily identical to the composition of the deposition solution (see below).

4.1.1. Electrochemical characterization

Immediately after deposition the solution was replaced by pure 1N H₂SO₄ and cyclic voltammograms (CV) were recorded between 30 and 800 mV versus RHE at a sweep rate of 20 mV/s. Figs. 2a–2f show selected CVs from 6 electrodes. Since at potentials above 950 mV corrosion and loss of Ru were reported [24], we have avoided exceeding this limit. The structures of these CVs in pure electrolyte are determined by the adsorption and desorption of hydrogen and oxygen species. In contrast to the well-known CV of polycrystalline Pt (Fig. 2f) the Ru CV (Fig. 2a) shows a structureless hydrogen region and a higher current density between 400 and 800 mV. The latter is due to the adsorption of oxygen species on Ru at potentials as low as 250 mV [7]. The CVs of the alloys change rather slowly from pure Ru to pure Pt with increasing Pt content in the deposition solution. In fact, the CVs of the alloys are dominated by Ru-like structures up to relatively high amounts of Pt in the solution (see for example Fig. 2d). Note, that the current densities of the electrodes are not fully comparable, because of slightly different degrees of surface roughness.

Additionally, Figs. 2g–2i display three cyclic voltammograms after CO adsorption at 100 mV (first sweep: solid line, second sweep: dotted line) on pure Ru and pure Pt as well as on a PtRu4:6 alloy. In these experiments the electrode was held at 100 mV for 5 min in each case in order to equilibrate the electrode in the hydrogen region and to have a reproducible starting point. The electrolyte was then continuously exchanged by CO-saturated H₂SO₄ under potential control. A ten minute waiting period was observed for the displacement of hydrogen by

CO to be completed. Subsequently the cell was purged with CO-free H₂SO₄ until the CO was completely removed from the electrolyte, before the adsorbed CO was oxidized in the first anodic scan with a sweep rate of 20 mV/s. As a consequence of the hydrogen displacement by the adsorbed carbon monoxide the hydrogen oxidation current at the beginning of the scan is suppressed. The CO oxidation manifests itself by a more or less sharp peak whose peak potential and peak width depend on the electrode composition. On pure Ru a single broad oxidation peak at ~ 620 mV is found. Pt shows a narrow peak at ~ 720 mV and a more cathodic broad prepeak at ~ 440 mV. All alloys revealed only one narrow oxidation peak, as exemplified by Fig. 2h.

The peak potential was taken as an indicator for the catalytic activity of the electrode as will be discussed later.

4.1.2. Spectroscopic determination of surface composition

After this electrochemical characterization the potential was held at 50 mV and the sulfuric acid was replaced by millipore water to remove the electrolyte from the surface of the electrodes. The electrodes were emersed and transferred to the UHV chamber and XPS (Fig. 3) and LEIS (Fig. 7) were performed to characterize the composition of the as-deposited surfaces. As far as we know this has never been done before without intermediate contact to air. Fig. 3 shows clearly the evolution of the XPS 4f and 3d core level peaks of Pt and Ru, respectively, as a function of the composition of the deposition solution. The intensity of these XPS lines was converted into surface compositions (in molar fractions) after subtraction of a linear background and taking into account elemental sensitivity factors for the 4f and 3d lines of pure Pt and Ru films, respectively, measured during this study. No further model calculations of the relative intensities based on electron mean free path lengths and different composition profiles within the probing depth were undertaken, because more emphasis is placed on the LEIS derived surface compositions anyway owing to the higher surface sensitivity of this technique. During the LEIS measurements a non-negligible sputter effect was observed. This effect was utilized to remove most of the weakly bonded adsorbates (originating

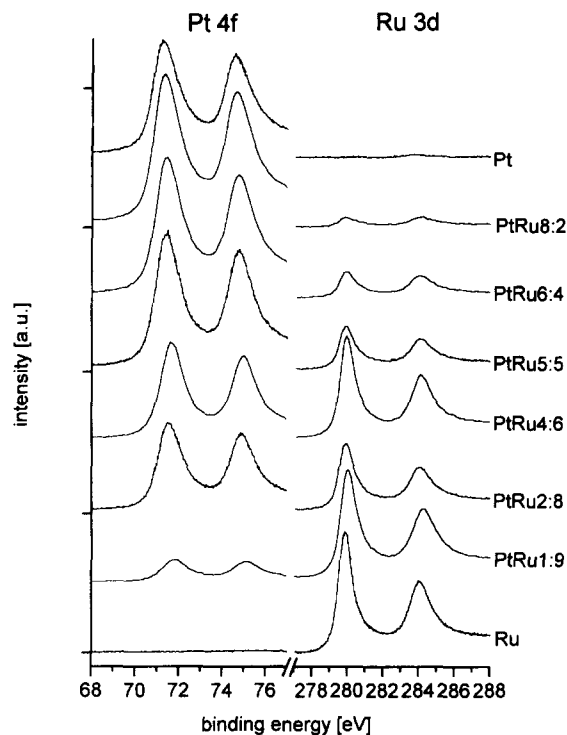


Fig. 3. XPS core level spectra of different PtRu alloys indicating the change in surface composition.

from the inner Helmholtz plane) before collecting the LEIS data. The LEIS measurements were quantified using Eq. (1) and standards of the pure metals measured during this study. The X_{Pt} of the surface compositions of the complete series of alloys as found with XPS and LEIS are summarized in Fig. 4. Four additional data points are added corresponding to electrodes, prepared under identical conditions, which were, however, not investigated electrochemically. Above 20 at% Pt in the solution a linear dependence of the surface composition on the solution composition exists (see straight solid line). Furthermore, the X_{Pt} at the surface is always higher than in the deposition solution, which will be discussed in Section 4.3. On the other hand, it has to be pointed out that the high concentration of Pt at the surface did not manifest itself in the CVs, whose shape was mainly determined by Ru (see Figs. 2a–2e).

4.2. Sputtered electrodes

4.2.1. Determination of surface composition

After the above described sequence of measurements the electrodes were sputtered with 2 keV argon ions until a constant X_{Pt} was reached in each case. These ratios are again displayed in Fig. 5 as a function of the concentration of the deposition solution from which the electrodes were originally prepared. Because of the nearly equal sputter yields for Pt and Ru ([14], and references therein) these ratios are close to the *bulk composition* of the electrodes. Again a linear dependence is found above concentrations of 20% Pt in the solution. Compared to the deposition solution, there is still a Pt enrichment, but to a lesser extent than at the surface before sputtering. This effect is the more pronounced the smaller the Pt content in the alloy is (as can be seen by comparison of the slopes of the solid lines in Fig. 4 and 5).

4.2.2. Electrochemical characterization

The freshly sputtered electrodes were transferred back to the high pressure chamber and were electrochemically investigated analogous to the as-de-

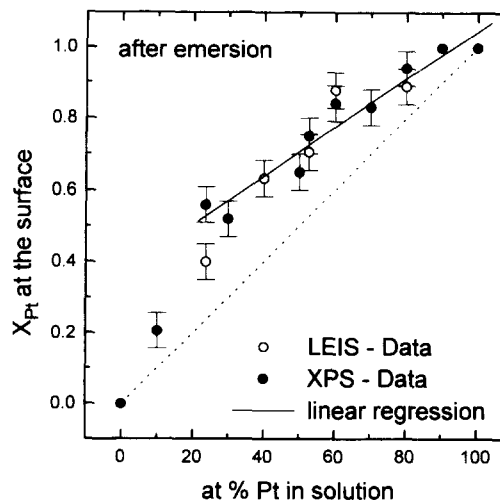


Fig. 4. Surface composition of different PtRu alloys as determined by XPS and LEIS after emersion from the electrolyte. Note the Pt surface enrichment compared to the Pt concentration in the solution (represented by the dotted line). The linear regression is only done in the fcc regime of the alloys (see text).

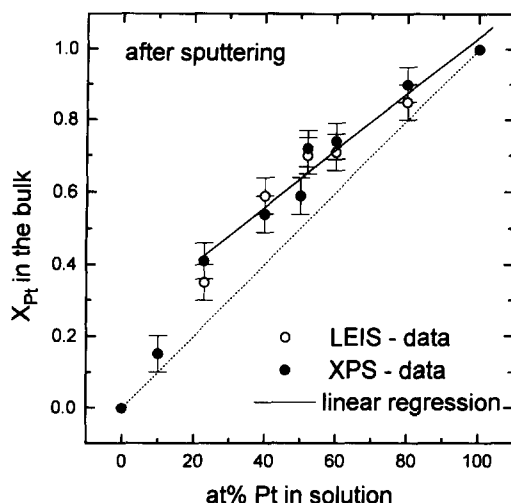


Fig. 5. Surface composition of different PtRu alloys as determined by XPS and LEIS after sputtering to a constant value, thus nearly representing the bulk concentration (see text). Note the Pt bulk enrichment compared to the Pt concentration in the solution (represented by the dotted line). The linear regression is only done in the fcc regime of the alloys (see text).

posited electrodes. They exhibited a very similar behavior with respect to the width and the number of CO oxidation peaks and the shape of the basic CVs (as shown in Figs. 2a–2i). Only the current densities of the sputtered electrodes were systematically lower, probably due to a smoothing of the initially very rough surfaces during sputtering with argon ions.

4.3. Further characterization of the electrodes

In the previous sections we found the sequence $X_{\text{Pt}}(\text{surface}) > X_{\text{Pt}}(\text{bulk}) > X_{\text{Pt}}(\text{solution})$ for the Pt concentration at the surface, in the bulk and in the deposition solution, respectively. In the following we will examine further the deposits, i.e. the enriched surface layer and the question as to why the bulk Pt content of the electrodes exceeds that of the deposition solutions. Even though both methods, XPS and LEIS, have a rather different information depth, both techniques yield the same Pt surface concentration (see Fig. 4). From this we tend to conclude that the first 4–5 layers corresponding to the information depth of the XPS spectra under the chosen experimental conditions are enriched with Pt. Any more

complicated (e.g. oscillatory) concentration profile from the surface into the bulk is difficult to visualize because the composition of the very surface is given by the LEIS data. Also sputter experiments did show a continuous decrease of the Pt concentration without compositional oscillations. In contrast, using atom probe measurements on annealed PtRu alloys Tsong et al. [20] reported a strong enrichment of Pt in the first and of Ru in the second layer. It has to be pointed out, however, that alloy samples annealed at high temperature in UHV (see Gasteiger et al. [14] and Tsong et al. [20]) and electrochemically deposited alloy films need not be comparable. We believe that the thickness of the Pt-enriched layer of the present samples is a peculiarity of the electrochemical preparation process. In any case, the composition of the outer surface is confirmed by the LEIS data.

A further observation is interesting to note. The XPS spectrum of the as-deposited PtRu4:6 electrode

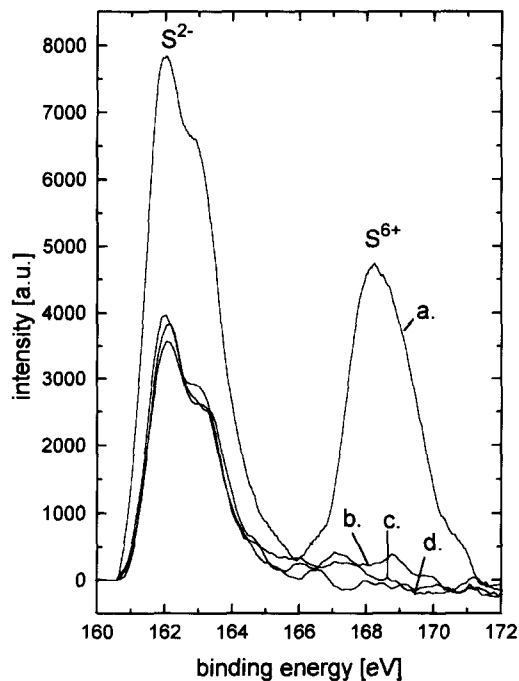


Fig. 6. Sulfur 2s core level emission measured with XPS. (a) Electrode after emersion (detection angle $\alpha = 50^\circ$ off normal). (b) Electrode after sputtering ($\alpha = 50^\circ$). (c) Electrode after sputtering ($\alpha = 0^\circ$). (d) Electrode after sputtering ($\alpha = 70^\circ$).

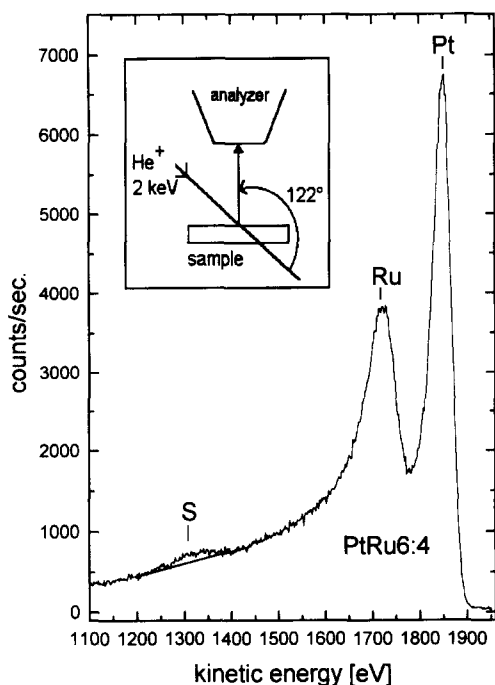


Fig. 7. LEIS spectrum of a sputtered PtRu4:6 alloy, showing a not negligible amount of sulfur in the surface. The inset refers to the experimental setup of the LEIS measurements.

shows two signals of sulfur 2s emission (Fig. 6, curve a), whose binding energies are characteristic for sulfate (SO_4^{2-}) and sulfide (S^{2-}), respectively. The sulfate (SO_4^{2-}) was found only after emersion and only on electrodes of the pure metals or of alloys with *high contents* of either Pt or Ru. This species, however is completely removed during the early stages of a LEIS experiment or during sputtering (see Fig. 6, curves b–d). By contrast, the sulfide is not removable during ion bombardment (see Fig. 6, curves b–d and Fig. 7) and is found with every deposit. Obviously the sulfide (S^{2-}) is built into the bulk of the electrode *during deposition*. This could be additionally verified by a variation of the detection angle in the XPS measurements (Fig. 6, curves b–d), which showed no angle dependence and, thus, no depth variation of the sulfide concentration. The presence of the sulfide however, is *certainly not* responsible for the Pt surface enrichment, because the heat of formation of Ru-sulfide is at least twice as large as that of Pt-sulfide.

4.4. Electrocatalytic properties

In this last section we investigate the electrocatalytic properties of the PtRu electrodes with respect to their CO oxidation activity. Taking the potential at the position of the CO oxidation peak as a measure of the catalytic activity, we have plotted in Fig. 8 these values for all characterized electrodes, either as-deposited or sputtered, as a function of their LEIS- (and XPS-) derived surface composition. As can be seen, the peak potential remains basically constant at the value typical for pure Ru (625 mV) up to a surface concentration of 40% Pt. Only then a sharp decrease occurs towards a minimum (500 mV) near 50% Pt, beyond which the oxidation (peak) potential steadily reincreases towards the value on pure Pt (720 mV). In Fig. 8 the data point at $\sim 40\%$ Pt happens to refer to a sputtered surface. It shall be emphasized, however, that the same steep decrease between $\sim 40\%$ and $\sim 50\%$ Pt was also detected with two as-deposited electrodes. Since the latter measurements were carried out with a slightly different sweep rate, i.e. 10 mV/s, these data are not included in Fig. 8.

According to the model of the bifunctional mechanism as proposed by Watanabe and Motoo [6] for the methanol oxidation on these alloys Ru adsorbs

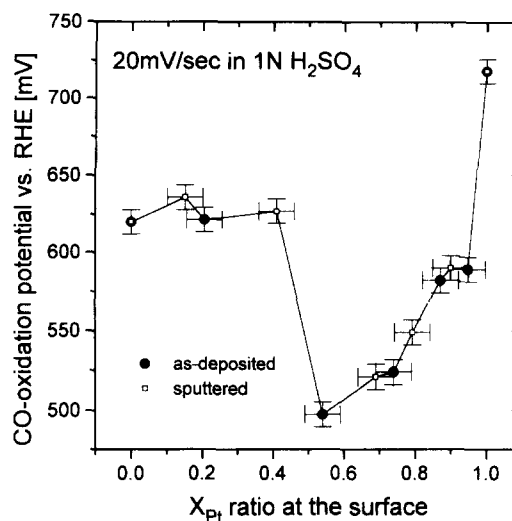
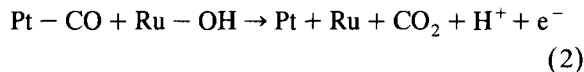


Fig. 8. Plot of the peak potential of the CO oxidation versus the X_{Pt} at the surface, i.e. “activity curve” of CO electrooxidation at PtRu surfaces.

the oxygen-containing species (e.g. OH) at much lower potential (compared to Pt), while a CO–Pt interaction provides a much faster reaction path (lower activation energy) for the CO oxidation to CO₂ (compared to Ru). Obviously, for the reaction



to occur, CO and OH should be absorbed on adjacent Pt and Ru sites, respectively. Hence the distribution of the two metal species in the electrode surface is of crucial importance. In the simplest model assuming a statistical distribution of Pt and Ru sites in the surface the “activity curve”, oxidation (peak) potential versus surface composition, should be more or less symmetric about the 50:50 composition (neglecting the difference between the potentials on both pure metals). The decrease in activity, i.e. the increase of the oxidation (peak) potential, on either side of this surface composition would be due to the lack of one or the other kind of adsorption sites, i.e. Ru or Pt, respectively. The obvious asymmetry of our measured “activity curve” in Fig. 8 conflicts either with the bifunctional reaction mechanism or with a statistical distribution of the Pt and Ru surface atoms (or both). We tend to assume the validity of the bifunctional mechanism and to suggest a non-statistical distribution of the Pt and Ru surface sites. This suggestion is based on the observation that the surface concentration of 40% Pt, at which we detect the abrupt decrease in the CO oxidation (peak) potential (see Fig. 8), coincides with the phase boundary between the single-fcc-phase and the two-(fcc/hcp)-phase regime in the PtRu phase diagram (Fig. 1). We are well aware that the phase diagram holds for temperatures above 1000°C, while all our depositions and measurements took place at room temperature. Nevertheless, *during* electrodeposition from the solution the mobility of the metal ions appears to be high enough to establish an equilibrium-like structure at the surface of the alloys (in agreement with earlier findings [25]), leading to some lateral segregation of Ru-rich and Pt-rich surface patches in the two-phase regime below a surface concentration of ~40% Pt. Of course, the verification of this explanation of the asymmetry of our ‘activity curve’ in Fig. 8 based on a surface struc-

tural phase separation as a function of surface composition would have to come from direct measurements with structure sensitive methods like TEM or STM.

5. Summary

In this work we have prepared and characterized a large number of PtRu electrodes in the same apparatus under air-free conditions, using both, electrochemical and surface science methods. The electrodes were prepared by electrochemical codeposition of Pt and Ru onto a Au foil from solutions containing variable concentrations of H₂PtCl₆ and RuCl₃ to a thickness of several μm. The as-deposited electrodes were first characterized by monitoring cyclic voltammograms in both, CO-free and CO-saturated 1N H₂SO₄. The *surface* composition of these electrodes was then determined by XPS and LEIS after sample transfer into an adjacent UHV chamber. Subsequent sputtering resulted in new surface compositions (corresponding approximately to the bulk composition of the deposited alloy films) which were again determined with XPS and LEIS and which, after reimmersion, were again used for cyclovoltammetric measurements with and without CO. In this way 12 different surface compositions could be related with the electrochemical properties of these PtRu alloy electrodes. It is this large number of different surface compositions as well as the fact, that none of the electrodes ever got into contact with air, which enables us to arrive at more systematic and firmer statements about this electrode system than any earlier work. We come to the following conclusions. Electrochemical codeposition of Pt and Ru from solution leads to PtRu films, which are always Pt enriched in the bulk and even more so at the surface. The surface enrichment (compared to the film bulk) suggests just sufficient surface mobility of the metal ions during deposition to cause surface segregation even at room temperature. The catalytic activity of these alloys in terms of their (peak) potential for electrooxidation of CO varies strongly with the surface composition. While this oxidation (peak) potential is nearly constant (and equal to the value from pure Ru) up to a surface concentration of ~40% Pt it drops abruptly beyond this concentra-

tion by 125 mV, going through a minimum near 50% Pt in the surface. It reincreased beyond this minimum steadily towards the value on pure Pt. Assuming the validity of the bifunctional reaction mechanism put forward by Watanabe and Motoo [6], we tentatively ascribe the asymmetry of our “activity curve” in terms of a structural phase separation at the surface in accordance with the phase diagram of the PtRu alloy system. The above mentioned high surface mobility during electrodeposition could facilitate this phase separation even at room temperature [25]. Affirmation of this proposal, however, would have to come from direct surface and bulk structure determinations.

Acknowledgements

We would like to thank the Institut für Energieverfahrenstechnik of the KFA Jülich for financial support. Without the patient and qualified help from P. Königshoven, M. Böhmer and G. Bermes with the development of the apparatus used in this studies this work would not have been possible. We wish to thank Ch. Stuhlmann for stimulating discussions.

References

- [1] R. Parsons and T. VanderNoot, *J. Electroanal. Chem.* 257 (1988) 9, and references therein.
- [2] V.M. Schmidt, P. Bröckerhoff, B. Höhlein, R. Menzer and U. Stimming, *J. Power Sources* 49 (1994) 229.
- [3] P.N. Ross, K. Kinoshita, A.J. Scarpellino and P. Stonehart, *J. Electroanal. Chem.* 63 (1975) 97.
- [4] V.B. Hughes and R. Miles, *J. Electroanal. Chem.* 145 (1983) 87.
- [5] J.O'M. Bockris and H. Wroblowa, *J. Electroanal. Chem.* 7 (1964) 428.
- [6] M. Watanabe and S. Motoo, *J. Electroanal. Chem.* 60 (1975) 267.
- [7] E. Ticanelli, J.G. Beery, M.T. Paffett and S. Gottesfeld, *J. Electroanal. Chem.* 258 (1989) 61.
- [8] T. Iwasita, F.C. Nart and W. Vielstich, *Ber. Bunsenges. Phys. Chem.* 94 (1990) 1030.
- [9] A. Hamnett and B.J. Kennedy, *Electrochim. Acta* 33 (1988) 1613.
- [10] M.A. Quiroz, I. Gonzalez, Y. Meas, E. Lamy-Pitara and J. Barbier, *Electrochim. Acta* 32 (1987) 289.
- [11] S. Szabo and I. Bakos, *J. Electroanal. Chem.* 230 (1987) 233.
- [12] L. Hilaire, G. Diaz Guerrero, P. Legare, G. Maire and G. Krill, *Surf. Sci.* 146 (1984) 569.
- [13] B.D. McNicol and R.T. Short, *J. Electroanal. Chem.* 92 (1978) 115.
- [14] H.A. Gasteiger, P.N. Ross, Jr. and E.J. Cairns, *Surf. Sci.* 293 (1993) 67.
- [15] H.A. Gasteiger, N. Markovic, P.N. Ross, Jr. and E.J. Cairns, *J. Phys. Chem.* 97 (1993) 12020.
- [16] H.A. Gasteiger, N. Markovic, P.N. Ross, Jr. and E.J. Cairns, *J. Phys. Chem.* 98 (1994) 617.
- [17] H.A. Gasteiger, N. Markovic, P.N. Ross, Jr. and E.J. Cairns, *Electrochim. Acta* 39 (1994) 1825.
- [18] H.A. Gasteiger, N. Markovic, P.N. Ross, Jr. and E.J. Cairns, *J. Electrochem. Soc.* 141 (1994) 1795.
- [19] B.D. McNicol and R.T. Short, *J. Electroanal. Chem.* 81 (1977) 249.
- [20] T.T. Tsong, D.M. Ren and M. Ahmad, *Phys. Rev. B* 38 (1988) 7428.
- [21] J.M. Hutchinson, *Plat. Met. Rev.* 16 (1972) 88.
- [22] J. Willsau and J. Heitbaum, *J. Electroanal. Chem.* 161 (1984) 93.
- [23] H. Nisch, W. Heiland and E. Taglauer, *Surf. Sci. Rep.* 17 (1993) 213.
- [24] R. Kötz, H.J. Lewerenz, P. Brüesch and S. Stucki, *J. Electroanal. Chem.* 150 (1983) 209.
- [25] E. Raub, *Metalloberfläche A* 7 (1953) 17.